Received: 30 January 2018 | Revised: 18 May 2018 | Accepted: 21 May 2018

DOI: 10.1002/pcr2.10011

WILEY Polymer Crystallization

FULL PAPER

# A novel numerical model for the interaction between the solidification front of a semicrystalline polymer and spherical particles

Eliana Agaliotis[1,2] | Analia Vazquez[1,2] | Celina Bernal[1,2]

[1]Universidad de Buenos Aires, Facultad de Ingeniería, Buenos Aires, Argentina

[2]CONICET-Universidad de Buenos Aires, Instituto de Tecnología en Polímeros y Nanotecnología (ITPN), C1127AAR, Buenos Aires, Argentina

**Correspondence**
CONICET-Universidad de Buenos Aires, Instituto de Tecnología en Polímeros y Nanotecnología (ITPN), Av. Las Heras 2214, C1127AAR, Buenos Aires, Argentina.
Email: eagaliotis@fi.uba.ar

**Funding information**
National Research Council of Argentina; University of Buenos Aires, Grant/Award Numbers: UBACYT 2014–2016, 20020130200282BA; 2017-2019, 20020160100055BA; FONCyT, Grant/Award Numbers: PICT 2014-1955, 2016-4543

## Abstract

The interaction between a solidification front of a semicrystalline polymer and a spherical particle is a topic of main interest because it addresses particle dispersion/distribution and materials behavior associated with this issue. In this paper, this interaction is investigated from numerical analyses by a computational fluid dynamics model that employs the shape of the interface to calculate drag and repulsion forces. The results obtained in turn are used to determine the conditions under which the particle is dragged by the solidification front. This is employed then to predict critical solidification front velocities for pushing as a function of particle size. The results shows that the numerical model developed here is able to accurately predict the conditions for particle pushing in semicrystalline polymers. The required cooling conditions which lead to a redistribution of the particles below 50 μm of radius during solidification in polymer composites and blends can be determined with the proposed model.

**KEYWORDS**

numerical modelling, semicrystalline polymers, solidification

## 1 | INTRODUCTION

Polymeric blends and composites are attractive materials due to their processability and wide applicability. Over the recent years considerable efforts have been devoted to obtain polymeric blends and composites with improved performance with respect to pristine polymers. They can be applied in different fields such as packaging, automotive parts, pipes, technical profiles and electronic components. During consolidation and forming processes the material properties can be modified by the presence of dispersed second phase particles, leading to either a positive or a negative effect.[1–6]

In the case of crystallizable composites and blends, the composition, molecular mass and crystallization conditions have a strong influence on their morphology, crystallization and thermal behavior.[1,2,7–11] One of the most commonly obtained morphology in polymers crystallizing from the melt is the spherulitic morphology which is formed by radially growing lamellar stacks.[12–15] Most of the studies reported in the literature on these materials are mainly focused on the crystallization kinetics of spherulites and on the effect of the second noncrystallizable component on the overall crystallization rate and polymer morphology.[7,16–21] Crystallization conditions are particularly important in determining the size, shape and degree of crystallinity and, for a given composition, could also affect second phase dispersion.[3–7,22–27] During slow cooling rates in semicrystalline polymers the dispersed second phase particles could be rejected from crystal to amorphous regions during the crystallization process. Hence, the material exhibits a nonhomogeneous distribution of particles, and therefore, it does not present a desirable final performance.[2–6,12]

Similar effects are also highly relevant in the presence of many antioxidants, u.v. stabilizers and other additives commonly incorporated into polymers. Several authors have reported the influence of

**Abbreviations:** $B_3$, Casimir–Lifshitz–Van der Waals constant = $6 \times 10^{-20}$ J; $\mu$, Viscosity; $R$, Particle radius; $F_d$, Drag Force; $F_r$, Repulsive Force; $h_{(r)}$, Particle–interface separation distance; $h_0$, the shortest interface-particle distance; $r$, Generic radius; $h_{min}$, Minimum particle-interface separation distance=$10^{-8}$ m; $h_{min}$, Equilibrium separation distance; $V$, Interface velocity; $V_{eq}$, Equilibrium velocity for pushing; $h_{eq}$, Equilibrium separation distance; $V_c$, Critical velocity for pushing

  

growing crystals on the pattern of the impurities that are excluded from the crystalline network. Moyer and Ochs demonstrated that polypropylene spherulites presented marked differences in the distribution of the tritiated additive, dilaurylthio-dipropionate.[28] In addition, Calvert and Ryan investigated the redistribution of antioxidants and u.v. absorbers in polypropylene.[29] Moreover, Keith and Padden showed that impurities were concentrated in the interlamellar amorphous regions and described how they affected the growth rate and morphology in high polymers like polypropylene and polystyrene.[9] Hence, the materials quality was found to be negatively affected. In some cases, when the particle acts as a nucleating agent, there is no rejection. Then, the study of the interaction between a solidification front of a semicrystalline polymer and a spherical particle addresses the conditions under which second-phase particles are pushed or engulfed by a solidifying interface, impacting over particle distribution/dispersion which is a topic of main interest.

The phenomenon of pushing has been extensively treated by Chernov et al.,[30] Bolling and Cisse,[31] Omenyi et al.[32] and later reviewed by Stefanescu.[33] The physical problem and the type of microstructure formed during crystallization depend on the thermo-physico-chemical properties of the material, the presence of impurities and the chemical composition or concentration of the phases and the external fields (gravity, thermal, and electromagnetic fields).[30–36] This problem does not still have a complete solution but all the theories include at least two forces: the drag and the repulsion forces.[30–37] The difference among these theories relies on how they assume the repulsion force. In all cases, particle–interface interaction strongly determines the distribution/dispersion of particles and consequently, affects the expected material properties. Although rejection or engulfing of the second component is a major factor in the crystallization of polymeric blends and composites, as stated before, the literature regarding this issue is still rather scarce.[4,5,12,38,39] Rejection of particles ahead of slow growing rate spherulites has been observed by several authors. [9,12,23,28,29,39–41] However, none of these studies was focused on the conditions under which rejection or pushing takes place in semicrystalline polymers. In these materials, melt viscosity, particle size, and hydrodynamic force are also major influencing factors in the particle rejection by the growing spherulites.

From experimental investigations on various organic and inorganic systems it has been demonstrated that there is a critical velocity of interface ($V_c$) at which the particle can no longer be pushed and is trapped and engulfed by the interface, leading to a good distribution of particles.[33]

Nevertheless, the critical velocity of pushing in a semicrystalline polymer containing second phase particles has not been already investigated. The literature about this topic only report the presence (or absence) of particle rejection by a growing spherulite.[9,12,28,29]

The aim of this work was to predict the critical velocity of pushing which leads to a particles redistribution on a semicrystalline polymer. The critical velocity is the only parameter experimentally measured which may be compared with those predicted by the model.

The model studied here is only valid for dilute systems and the particle size considered was up to 50 μm of radius. This assumptions were made taking into account that for larger particle sizes, critical velocities for pushing in polypropylene are extremely low and hence, they are not likely to occur for the geometrical configuration studied. This tendency has been reported before for other authors and other materials.[31,37,40,41]

On the other hand, this work is based on an analytical and numerical model previously developed for other materials which was also successfully contrasted with experimental observations.[42–46]

From this model, it was found that cooling rate is one of the main determining factors of particles distribution/dispersion in the material. These simulations are very useful to understand the rejection process and the effect of the solidification rate on particle distribution/dispersion and hence, to predict physical properties of polymeric parts and components.

The previously developed model was used here to predict the behavior of the filler (pushing) in a semicrystalline polymer for the first time combining the properties of the particle, the flow field and the solidification process.[42–46]

The development of a model able to estimate the critical conditions for pushing, particularly the critical velocity, will allow optimizing industrial processes to obtain a specific distribution/dispersion of second-phase particles. Hence, a deep knowledge of these critical conditions is essential to predict the material final performance.

## 2 | METHODS SECTION

### 2.1 | The pushing model

The model was applied to the solidification of a semicrystalline polymer, that is, isotactic polypropylene (iPP), containing a spherical particle immersed in the melt and the solidifying interface moving toward the particle. The aim of the model was to determine the critical conditions for particle pushing ahead the interface.

The model used is schematically shown in Figure 1. The solidification front was performed for the growth of a semicrystalline structure or a spherulite as a solidifying interface. The particle was firstly assumed to be spherical, but other particle shapes will be considered in future models. The physics of the problem is governed by a dynamic balance of forces.[30–47] Assuming a steady-state condition of pushing and neglecting the gravitational acceleration, the governing forces acting onto the particle were the drag and the repulsion forces.

#### 2.1.1 | Drag forces

Drag forces results for a spherical particle and a flat interface were previously calculated from the numerical analysis developed in a computational fluid dynamics model and originally presented in another report where was demonstrated that analytical expressions such as Stokes equation lost accuracy at values of particle–interface distance ($h$) smaller than $R$. This is the main reason to solve this problem by the model presented in this report.[48] In addition, drag forces corresponding to the configuration of a spherical particle and other two "convex interface" curvatures were determined. The fluid flow was assumed to be a viscous fluid polymer at zero shear viscosity. This condition was based on the results of Xu et al.[5] who reported that fluid flow can occur in an undercooled polymer melt during isothermal crystallization of iPP in the presence of a second phase (carbon black).

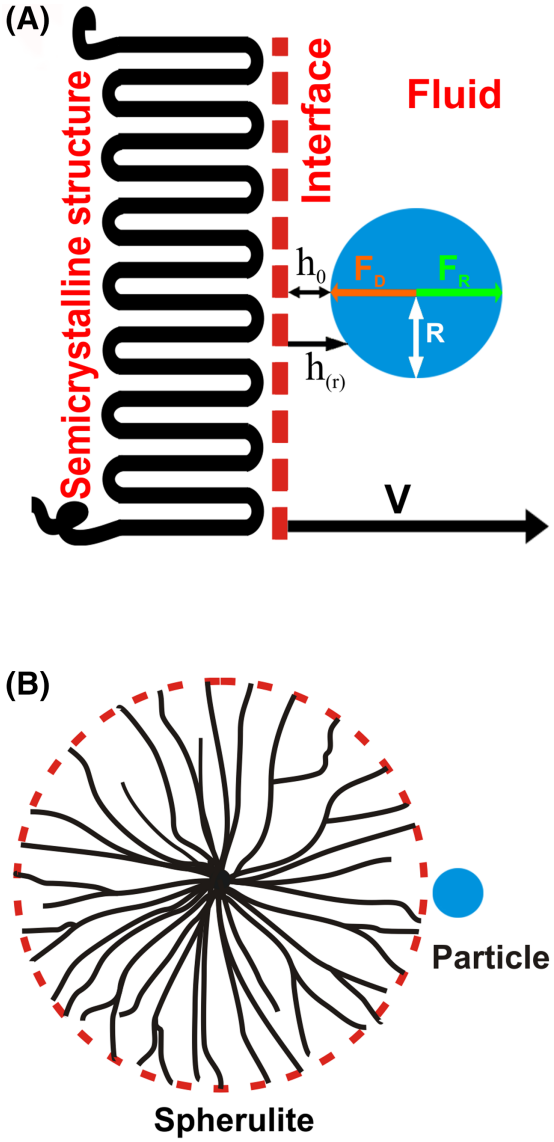


**FIGURE 1** (A) Scheme of the pushing model used where $F_d$ is the drag force, $F_r$ the repulsive force, $R$ the radius of the particle, $h(r)$ the interface-particle distance, and $V$ the velocity of the growing front, (B) Schematic representation of a particle being pushed by spherulitic growth front

The model was simulated on an axi-symmetrical domain using 30 000 and 50 000 quadrilateral elements, with second order interpolation functions for the velocity and first order for the pressure. The boundary conditions were: (i) constant fluid velocity in the surface taken as a sink, (ii) no-slip condition on the particle surface and (iii) other boundaries: free. Newtonian fluid in a laminar flow regime, ($Re \ll 1$). Several particle radii were simulated 0.001–50 μm.

Equations of conservation of mass and momentum were included in the numerical solutions of the problem. The resulting system of equations were solved by the Picard method.[49]

Full Navier Stokes equations were numerically solved from the velocity field by a finite element method in order to calculate drag forces onto the particle.

As it was shown, the drag force ($F_d$) strongly depends on the velocity and shape of the interface, and also on the distance between particle and interface.

The repulsive force model is based on the theory of Chernov et al.[30] and was calculated using the Lifshitz Van der Waals force equation taking into account the interface shape.

These two fields were coupled to analyze the conditions under which the particle could be pushed by the growing front and to predict critical velocities for pushing as a function of particle size.

The equilibrium point for steady state of pushing is obtained when both forces, $F_d$ and $F_r$, are equal.[33] The corresponding distance and velocity are: the equilibrium separation distance heq and the equilibrium velocity $V_{eq}$, respectively for steady state of pushing. The trapping condition applies when the separation distance between particle and interface reaches a minimum value of $h_{min} = 1 \times 10^{-8}$ m, which is assumed to be the minimum thickness for a film to be considered as fluid.[30,50,51] The above method of calculation has been already applied for other materials, and it was adjusted and tailored in this work for a viscous material as iPP.[42–46] From these results the equilibrium velocity and particle–interface distance for steady state of pushing were calculated.

### 2.1.2 | Repulsive forces

Repulsive forces were calculated from the Van der Waals force expression. Their influence in the pushing process may be strong enough to determine the pushing and capture process. The Casimir–Lifsitz–Van der Waals force (Equation 1) acts in many processes as in chemical flocculation, coagulation or agglomeration of particles and also between small particles interacting with themselves as in the solid–liquid interface. [27,52–59]

$$F_r = 2\pi B_3 \int_0^R \frac{r dr}{h^3(r)} \quad (1)$$

The Van der Waals force employed in the present calculations was proposed by Lifshitz et al.[58–61] This equation must be integrated for each geometrical configuration and in the case of a spherical particle and a flat interface can be written as it is shown in Equation 2.[37]

$$F_r = 2\pi B_3 \frac{R}{h_0^2} \quad (2)$$

Where $B_3$ is a Casimir–Lifshitz–Van der Waals constant, $h(r)$ is the separation distance between particle and interface, $h_0$ is the shortest interface–particle distance and $R$ is the particle radius as it is shown in Figure 1.

Equation 2 is applied to a system in which the film is not metallic and the sign of the parameter $B_3$ is negative in order to have pushing. The value of $B_3$ of $6 \times 10^{-20}$ J was selected from the values reported in the literature for similar systems.[30,57–59]

## 3 | RESULTS AND DISCUSSION

Drag forces depend on the particle radius, distance $h$ between particle and interface and interface velocity. Particle radii studied here were 1, 10, and 50 μm and interface velocity was from $1 \times 10^{-18}$ to $1 \times 10^{-9}$ m s$^{-1}$. Previous drag forces results were coupled with repulsive forces results (Equation 1) to calculate the equilibrium condition of pushing and the critical velocity at each particle radius.[48]

Repulsive forces results mainly depend on the distance between the particle and the interface $h$ and on the shape of the interface at each distance. In the case of a convex interface, two curvatures were added taking into account two radii for the spherulitic interface shape, $R_1$=10$R$, $R_2$=2$R$. Typical flow field results for these two curvatures are shown in Figure 2. The fluid flow was continuous around the particle with no separation lines and showed an increase of velocity in the narrow gap.

It was demonstrated that drag forces results from simulations in the case of a spherical particle and a flat interface could be calculated by an analytical equation only if particle size was lower than 100 μm and interface–particle distance was lower than 2$R$. Owing to that, the repulsive $F_r$ and drag $F_d$ forces are computed by simple expressions when the interface is flat by applying the Modified Stokes and the Casimir Lifshitz Van der Waals force (Equation 2).[48] Therefore, by equating these two analytical expressions, the equilibrium velocity ($V_{eq}$) and the equilibrium position distance ($h_{eq}$) at this velocity for steady state pushing can be easily computed as follows:

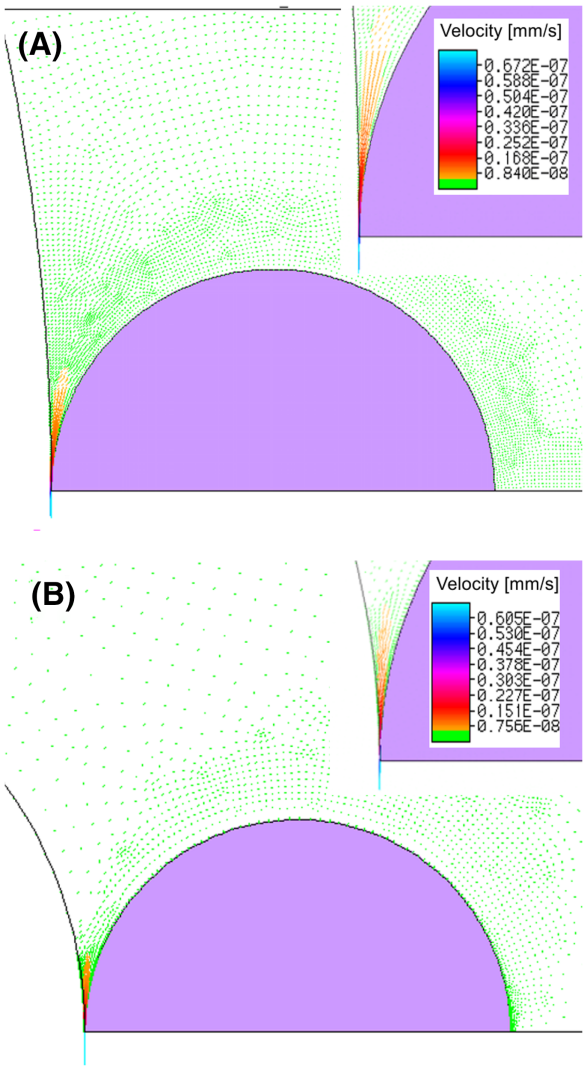


**FIGURE 2** Flow fluid results for a convex interface at $h = 1 \times 10^{-8}$ m, $R$ = 50 μm and $V = 2.1 \times 10^{-12}$ m s$^{-1}$ for two different radii of spherulite interface shape, (A) $R_1$=10$R$, (B) $R_2$=2$R$

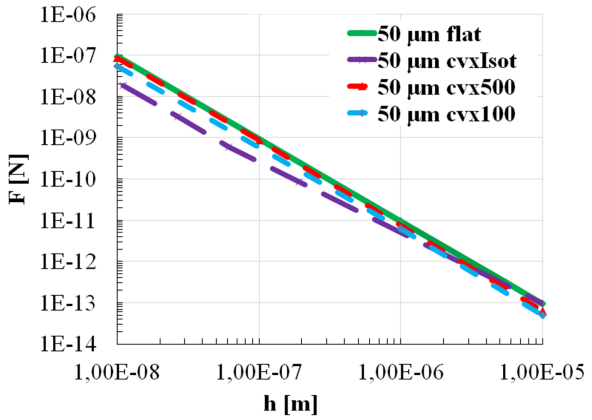


**FIGURE 3** Repulsive forces ($F_r$) as a function of the separation distance $h$ for a flat and convex ($R$ = 500, $R$ = 100 and isotherm shape) interface onto a particle 50 μm in radius

$$V_{eq} = \frac{B_3}{6\mu h_{eq} R} \quad (3)$$

Repulsive forces results for flat and convex interfaces and a particle of 50 μm were calculated by using Equation 2 and 1, respectively (Figure 3).These results showed that the higher the interface curvature, the smaller the repulsive force ($F_r$). On the other hand, the equilibrium velocity $V_{eq}$ was determined by the intersection points of $F_r$ and $F_d$ curves as it is shown in Figure 4 for a value of $h = 1 \times 10^{-8}$ and two cases: a flat interface and a convex interface (spherulite of $R$ = 500 μm), as an example.

This procedure was used to determine the equilibrium velocity $V_{eq}$ and the equilibrium distance $h_{eq}$ for each configuration and condition. These results were extrapolated to obtain the critical velocity $V_c$ and correspond to the velocity $V_{eq}$ at which the equilibrium distance is $h_{min}$=1 × 10$^{-8}$ m (the minimum thickness for a film to be considered as fluid).[30,50,51] If the velocity of the interface is higher than the critical velocity, there is no more pushing and the particle will be trapped by the solid. In our case, if the spherulitic growth rate is higher than that velocity, the particle will be engulfed by the solidifying front.

A good agreement between analytical (Equation 3) and FEM models was obtained for values of $h/2R$ less than 0.1 for a flat interface. On the other hand, a convex interface displayed higher values of

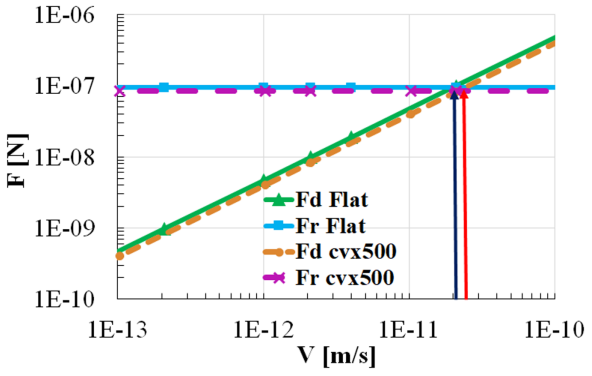


**FIGURE 4** Repulsive ($F_r$) and drag ($F_d$) forces as a function of the solidification velocity for a flat and convex interface at the interface–particle distance $h$ of 1 × 10$^{-8}$m. The intersection gives the equilibrium velocity ($V_{eq}$) for steady state particle pushing

**TABLE 1** Critical velocity of pushing at different particle radii for a zero shear viscosity of $1 \times 10^{+3}$ Pa s

| Particle radius (μm) | Critical velocity (μm $min^{-1}$) |
|---|---|
| 0.001 | 5.8 |
| 0.01 | 3 |
| 0.05 | 1 |
| 0.1 | 0.64 |
| 1 | 0.061 |
| 10 | 0.0064 |
| 50 | 0.00129 |

equilibrium velocity. These results showed that the higher the interface curvature, the higher is the difference with flat interface results. Therefore, critical velocities results also reflected this difference. Besides, for a given solidification velocity, the equilibrium distance increased as the particle radius decreased indicating that the critical growth velocity increased accordingly.

In addition, the values of critical velocities for a flat interface at each particle radius are shown in Table 1. As it is shown in this Table 1 and in Figure 5, the lower the particle radius, the higher the critical velocity value. Therefore, the odd of pushing these particles improves. Critical velocities results for a convex interface were calculated for particle radii of 50 μm and are shown also in Figure 6 and Table 2. In the case of convex interfaces, all critical velocities were smaller than for a flat interface pointing out that the higher the curvature, the higher is the probability for the particle of being pushed.

Significantly low values of critical velocities were obtained in this work, in agreement with experimental data for thin films of iPP unidirectionally solidified at a constant temperature gradient of 5.5 K $mm^{-1}$ (from 0.019 to 1.9 μm $s^{-1}$).[3,19,60,61] It has been reported in the literature that crystal growth rate (critical velocity) could be related to cooling conditions. For nonisothermal crystallization of PP with low cooling rates between 0.5 and 1 K/min, the spherulite growth rate was experimentally found to be below 20 μm/min.[62,63] In addition, for isothermal crystallization the range of spherulite growth rate experimentally measured was between 0.1 and 20 μm/min.[62–64] In the particular case of PP under isothermal conditions at 138 °C, Xu et al. also reported a similar range of spherulite growth rate (2–13 μm/min).[5]

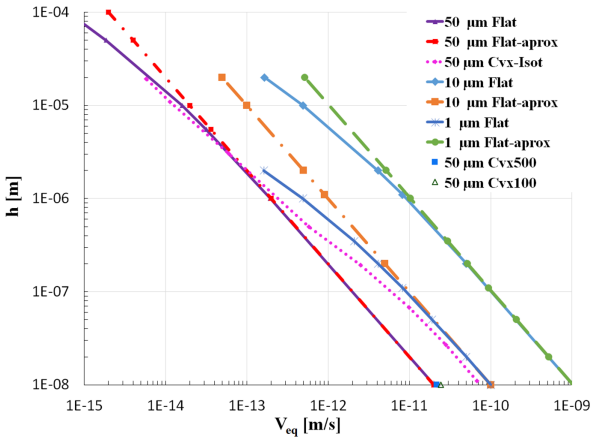


**FIGURE 5** Equilibrium separation distance for steady state of pushing as a function of the solidification velocity for a flat interface

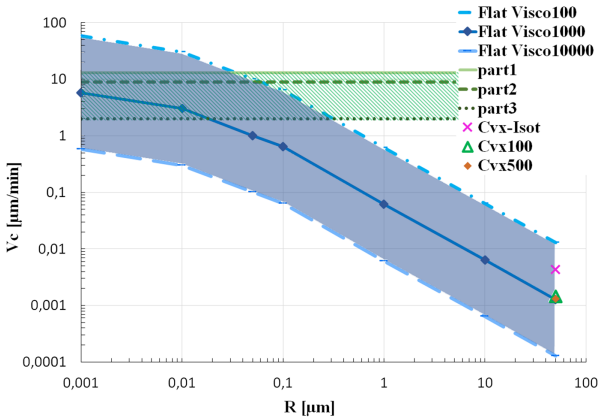


**FIGURE 6** Simulations results of critical velocity of pushing as a function of particle radii for a flat interface and three zero shear viscosities ($1 \times 10^{+2}$, $1 \times 10^{+3}$, and $1 \times 10^{+4}$ Pa s); for convex interfaces (for a zero shear viscosity of $1 \times 10^{+3}$ Pa s) and experimental results reported by Xu et al.[5] for three particles tracked

Finally $V_c$ values were also calculated for very small particle sizes (Figure 6) and compared with the experimental results reported by Xu et al.[5] for iPP filled with carbon black (CB). For an isothermal crystallization temperature of 138 °C, they observed that the size of the spherulites reached about 30–40 μm and the fastest recorded displacement rates of the CB particles were between 2.9 and 13 μm $min^{-1}$, being these particles rejected by the spherulites. The radius of the CB particles was smaller than 10 μm and the spherulite size was at least 10 times higher this radius. Taking all these into account, Xu et al. results could be approached to a flat interface. The recorded particles velocities are a little higher than those predicted in our model for zero shear viscosity of $1 \times 10^{+3}$Pa s, probably due to changes in the shear rate. It is well known that viscosity decreases with an increase of the shear rate viscosity. A decrease of the viscosity values increases the critical velocity for steady state particle pushing. In order to evaluate this, two viscosities ($1 \times 10^{+4}$ and $1 \times 10^{+2}$ Pa s) were simulated and critical velocity values were calculated. As it is shown in Figure 6, the results of our model are in agreement with those of Xu et al. for particles with radii smaller than 0.5 μm. The lowest size value for particles assumed here was 0.001 μm because at such very low particle sizes, the effect of Brownian motion will dominate the particle movement; and as a result it was expected that particles are engulfed rather than pushed. In addition, this effect becomes more relevant as particle size decreases. On the other hand, experimental validation of results will be almost impossible for these small particle sizes.[31,34,37,65]

**TABLE 2** Critical velocity of pushing for different interface shapes and $R$ = 50 μm for a zero shear viscosity of $1 \times 10^{+3}$ Pa s

| Shape Interface – $R$ = 50 (μm) | Critical velocity (μm $min^{-1}$) |
|---|---|
| Flat | 0.00129 |
| Cvx 500 | 0.00131 |
| Cvx 100 | 0.00146 |
| CvxIsot | 0.00433 |

At the time of writing and to the author's knowledge, critical velocity values for particle pushing in semicrystalline polymers have not been previously reported. The current model was certainly used for spherical particles as it is the simplest approximation to predict the critical velocities for particle pushing in a solidifying semicrystalline polymer. However, the development of this approximation is still time consuming.

Predictions obtained here will be considered for further models development in the case of other particle geometries by taking into account these results as reference data

## 4 | CONCLUSIONS

The interaction between a solidification front of a semicrystalline polymer and a spherical particle was numerically simulated. From the results obtained in this investigation, the following conclusions can be drawn.

Critical velocity for steady state particle pushing was accurately predicted and calculated for a flat interface and a spherical particle from 0.001 to 50 μm of radii in a polymeric matrix. Good agreement between analytical and numerical models was obtained for values of $h/2R$ less than 0.1, where $h$ is the distance between interface and particle and $R$ is the radius of the particle.

Critical velocity ($V_c$) values decreased with the increase of particle size. In addition, $V_c$ values for a convex interface were smaller than for a flat interface pointing out that the higher the curvature, the higher is the probability for the particle of being pushed.

From the results obtained here, it was confirmed that the proposed model is able to accurately predict critical velocity values for particle pushing and hence, the cooling conditions which lead to a redistribution of the particles in a dilute system during solidification and consequently modify the material final performance. A deep knowledge of this phenomenon has very important implications to optimize industrial processes of semicrystalline polymers in order to obtain the desired material.

### ACKNOWLEDGMENTS

The authors want to thank the National Research Council of Argentina, the University of Buenos Aires (UBACYT 2014–2016, 20020130200282BA; 2017-2019, 20020160100055BA) and the FONCyT (PICT 2014-1955; 2016-4543) for financial support of this investigation.

### REFERENCES

[1] J. Karger-Kocsis, T. Bárány, *Compos. Sci. Technol.* **2014**, *92*, 77.
[2] J. Karger-Kocsis, *Polypropylene Structure, Blends and Composites: Volume 3 Composites*, Springer, Berlin **2012**.
[3] D. W. Van Krevelen, K. Te Nijenhuis, *Properties of Polymers: Their Correlation with Chemical Structure; Their Numerical Estimation and Prediction from Additive Group Contributions*, Elsevier, Boston, **2009**.
[4] E. Martuscelli, *Polym. Eng. Sci.* **1984**, *24*, 563.
[5] D. Xu, Z. Wang, J. F. Douglas, *Macromolecules* **2007**, *40*, 1799.
[6] I. Kindgren. Master of Science Thesis. Chalmers University of Technology. Maskingränd 2, 412 58 Göteborg, Suecia, Report No. 409, **2012**.
[7] L. Mandelkern, *Crystallization of Polymers: Volume 2, Kinetics and Mechanisms*, Cambridge University Press, Cambridge **2004**.
[8] H. D. Keith, F. J. Padden, *J. Appl. Phys.* **1963**, *34*, 2409.
[9] H. D. Keith, F. J. Padden, *J. Appl. Phys.* **1964**, *35*, 1270.
[10] D. C. Bassett, *J. Macromol. Sci. Part B Phys.* **2003**; *42 B*, 227.
[11] B. Wunderlich, *Thermal Analysis of Polymeric Materials*. Springer, Berlin **2005**.
[12] M. L. Di Lorenzo, *Prog. Polym. Sci.* **2003**, *28*, 663.
[13] J. Varga, *Macromol. Mater. Eng.* **1983**, *112*, 161.
[14] C. Buckley, J. M. Schultz, *Prog. Polym. Sci.* **2016**, *56*, 1.
[15] R. H. Olley, D. C. Bassett, *Polymer* **1989**, *30*, 399.
[16] A. Pawlak, E. Piorkowska, *Colloid Polym. Sci.* **2001**, *279*, 939.
[17] A. G. Shtukenberg, Y.O. Punin, E. Gunn, B. Kahr, *Chem. Rev.* **2012**, *112*, 1805.
[18] B. Dimzoski, I. Fortelný, M. Šlouf, A. Sikora, D. Michálková, *Polym. Bull.* **2013**, *70*, 263.
[19] P. Smith, A. J. Pennings, *Eur. Polym. J.* **1976**, *12*, 781.
[20] J. Kang, B. Wang, H. Peng, J. Chen, Y. Cao, H. Li, M. Xiang, *Polym. Bull.* **2014**, *71*, 563.
[21] M. G. Ahangari, A. Fereidoon, N. Kordani, H. Garmabi, *Polym. Bull.* **2011**, *66*, 239.
[22] A. Durin, J. L. Chenot, J. M. Haudin, N. Boyard, J. L. Bailleul, *Eur. Polym. J.* **2015**, *73*, 1.
[23] A. Toda, R. Androsch, C. Schick, *Polymer* **2016**, *91*, 239.
[24] H. E. Oktay, E. Gürses, *Mech. Mater.* **2015**, *90*, 83.
[25] L. Mandelkern, *Crystallization of polymers*, McGraw-Hill, New York **1964**.
[26] J. Varga, *Polypropyl. Struct. blends Compos.* **1995**, *1*, 56.
[27] M. L. Di Lorenzo, C. Silvestre, *Prog. Polym. Sci.* **1999**, *24*, 917.
[28] J. D. Moyer, R. J. Ochs, *Science.* **1963**, *142*, 1316.
[29] P. D. Calvert, T. G. Ryan, *Polymer.* **1978**, *19*, 611.
[30] A. A. Chernov and T.E. Temkin, in *Crystal Growth and Materials* (Eds.: E. Kaldis, H. J. Sheel), North Holland, Amsterdan **1977**.
[31] G. F. Bolling, J. Cisse, *J. Cryst. Growth.* **1971**, *10*, 56.
[32] S. N. Omenyi, A. W. Neumann, W. W. Martin, G. M. Lespinard, R. P. Smith, *J Appl. Phys.* **1981**, *52*, 796.
[33] D. M. Stefanescu, *Trans. Indian Inst. Met.* **2007**, *60*, 79.
[34] A. V. Catalina, S. Mukherjee, D. Stefanescu, *Metall. Mater. Trans. A* **2000**, *31*, 2559.
[35] D. R. Uhlmann, B. Chalmers, K. A. Jackson, *J. Appl. Phys.* **1964**, *35*, 2986.
[36] J. K. Kim, P. K. Rohatgi, *Acta Mater.* **1998**, *46*, 1115.
[37] C. E. Schvezov, *Solidification 1999*, Proceedings of Symposia Sponsored by the Solidification Committee of the Materials Processing & Manufacturing Division of Tms, Held in Rosemont, Published by Minerals, Metals, & Materials Society, **1999**, ISBN 10: 0873394291/ISBN 13: 9780873394291, p. 251.
[38] R. A. Register, *ACS Cent Sci.* **2017**, *3*, 689.
[39] Z. Bartczak, A, Gałęski, E. Martuscelli, *Polym. Eng. Sci*, **1984**, *24*, 1155.
[40] D.M. Stefanescu, A. Catalina, F. Juretzko, S. Mukherjee, S. Sen, & B. Dhindaw, *Proc. First Int. Symp.* (10–15 September 2000), Sorrento (Italy). ESA SP-454, **2001**, 621
[41] H. Aufgebauer, J. Kundin, H. Emmerich, M. Azizi, C. Reimann, J. Friedrich, T. Jauß, T. Sorgenfrei and A. Cröll, *J. Cryst. Growth*, **2016**, *446*, 12.
[42] E. Agaliotis, M. R. Rosenberger, C. E. Schvezov, A. E. Ares, *J. Cryst. Growth* **2008**, *310*, 1366.
[43] E. M. Agaliotis, M. R. Rosenberger, A. E. Ares, C. E. Schvezov, *Procedia Mater Sci.* **2008**, *1*, 58.
[44] E. M. Agaliotis, C. E. Schvezov, M. R. Rosenberger, A. E. Ares, *J. Cryst. Growth* **2012**, *354*, 49.
[45] E. M. Agaliotis, M. R. Rosenberger, A. E. Ares, C. E. Schvezov, *RSC Adv. R. Soc. Chem.* **2012**, *2*, 12000.
[46] E. M. Agaliotis, M. R. Rosenberger, A. E. Ares, C. E. Schvezov, *CFD Modeling and Simulation in Materials*, TMS (The Minerals, Metals & Materials Society), Pittsburgh **2012**, 171.
[47] Y. Tao, A. Yeckel, J. J. Derby, *J. Comput. Phys.* **2016**, *315*, 238.
[48] E. Agaliotis, C. Bernal, *Colloid Interface Sci. Commun.* **2017**, *19*, 20.
[49] S. C. Chapra, R. P. Canale, *Numerical Methods for Engineers*. McGraw-Hill, New York **2012**.
[50] K. V. Sharp, R. J. Adrian, *Exp. Fluids* **2004**, *36*,741.

[51] K. P. Travis, B. D. Todd, D. J. Evans, *Phys. Rev.* **1997**, *E 55*, 4288.
[52] I. E. Dzyaloshinskii, E. M. Lifshitz, L. P. Pitaevskii, *Physics-Uspekhi.* **1961**, *4*,153.
[53] B. A. Rozenberg, R. Tenne, *Prog. Polym. Sci.* **2008**, *33*, 40.
[54] L. Belloni, *J. Phys. Condens Matter*. **2000**, *12*, R549.
[55] H. Krupp, G. Walter, W. Kling, H. Lange, *J. Colloid Interface Sci.* **1968**, *28*, 170.
[56] H. Krupp, W. Schnabel, G. Walter, *J. Colloid Interface Sci.* **1972**, *39*, 421.
[57] M.P. Howard, S.T. Milner, *Macromolecules.* **2013**, *46*, 6600.
[58] E. M. Lifshitz, *Sov. Phys.* **1956**, *2*, 73.
[59] J. Vial, A. Carré, *Int. J. Adhes. Adhes.* **1991**, *11*, 140.
[60] S. Anantawaraskul, J. B. P. Soares, P. M. Wood-Adams, *Adv. Polym. Sci.* **2005**, *182*, 1.
[61] T. Huang, A. D. Rey, M. R. Kamal, *Polymer*. **1994**, *35*, 5434.
[62] Y. Shangguan, Y. Song, Q. Zheng, *Polymer*, **2007**, *48*, 4567.
[63] Q. Zheng, Y. Shangguan, S. Yan, Y. Song, M. Peng, Q. Zhang, *Polymer* **2005**, *46*, 3163.
[64] F. J. Padden Jr, and H. D. Keith, *J. Appl. Phys.* **1959**, *30*, 1479.
[65] J. Q. Xu, L. Y. Chen, H. Choi, X. C. Li, *J. Phys. Condens. Matter* **2012**, *24*, 255304.

**How to cite this article:** Agaliotis E, Vazquez A, Bernal C. A novel numerical model for the interaction between the solidification front of a semicrystalline polymer and spherical particles. *Polymer Crystallization*. 2018;1:e10011. https://doi.org/10.1002/pcr2.10011